Using inverse transmission matrices for Marchenko redatuming in highly complex media

Ivan Vasconcelos, Schlumberger; Kees Wapenaar and Joost van der Neut, Delft University of Technology; Colin Thomson, Schlumberger; and Matteo Ravasi, University of Edinburgh.

Summary

The goal of Marchenko redatuming is to reconstruct, from single-sided reflection data, wavefields at virtual subsurface locations containing transmitted and reflected primaries and internal multiples, while relying on limited or no knowledge of discontinuties in subsurface properties. Here, we address the limitations of the current Marchenko scheme in retrieving waves in highly heterogeneous media, such as subsalt or sub-basalt. We focus on the initial focusing function that plays a key role in the iterative scheme, and propose an alternative focusing function that uses an estimate of the inverse transmission operator from a reference model that contains sharp contrasts (e.g., salt boundaries). Using a physics-driven estimate of the inverse transmission operator, we demonstrate that the new approach retrieves improved subsurface wavefields, including enhanced amplitudes and internal multiples, in a subsalt environment.

Introduction

The retrieval of wavefields within the earth's subsurface where no receivers or sources are available is a key component of wave-equation imaging and inversion; however, retrieving full-wave responses containing internal multiples with improved amplitudes has long presented a challenge to imaging practice. The method of Marchenko redatuming or autofocusing (Broggini et al., 2011; Wapenaar et al., 2013) proposes to retrieve such wave responses inside the subsurface, while using relatively little information about the earth's properties. The fields retrieved by Marchenko redatuming can, in principle, be used to improve imaging beyond current capabilities, as discussed by Behura et al. (2012), van der Neut et al. (2013), Broggini et al. (2014), Slob et al. (2014),Wapenaar et al. (2014a) and Vasconcelos et al. (2014). Recently, Ravasi et al. (2015) validated the imaging capabilities of the method on ocean-bottom field data. While indeed capable of retrieving internal multiples and correcting amplitudes, recent studies in the presence of highly complex media brought forth some limitations of the current Marchenko scheme (van der Neut et al., 2014a; Wapenaar et al., 2014b). With the aim of applying Marchenko redatuming in geologically complex media such as subsalt, we review the limitations of the existing approach and propose an alternative scheme capable of accounting for higher medium complexity.

Marchenko redatuming

The underlying equations of Marchenko redatuming (Wapenaar et al., 2013, 2014a) can be compactly written in discrete-matrix form as (van der Neut et al., 2014b)

$$\mathbf{G}^- + \mathbf{F}_1^- = \mathbf{R}\,\mathbf{F}_1^+ \,, \tag{1}$$

and

$$\mathbf{G}^{+\star} + \mathbf{F}_1^+ = \mathbf{R}^\star\,\mathbf{F}_1^- \,, \tag{2}$$

where the matrices $\mathbf{G}^-$ and $\mathbf{G}^+$ contain the Green's functions due to sources at every point on the surface $\partial \mathbb{D}_0$, which are respectively either up- or downgoing at all receiver locations on an arbitrary datum at depth $\partial \mathbb{D}_a$ (Figure 1). The $\star$ superscript denotes time-reversed fields; here, we assume equations to be in the frequency domain, although the form of the Marchenko equations is the same in the time domain. The $\mathbf{R}$ matrix is the reflection response of the medium due to sources and receivers on the surface $\partial \mathbb{D}_0$ and acts as a multidimensional convolution operator in the Marchenko system (e.g., van der Neut et al., 2014b; Wapenaar et al., 2014a). The focusing functions $\mathbf{F}_1^+$ and $\mathbf{F}_1^-$ are key to the Marchenko formulation, with, by definition,

$$\mathbf{I} = \mathbf{T}_A\,\mathbf{F}_1^+ \tag{3}$$

and $\mathbf{F}_1^- = \mathbf{R}_A\mathbf{F}_1^+$, where $\mathbf{R}_A$ and $\mathbf{T}_A$ are the full reflection and transmission responses for a medium that is truncated between the surfaces $\partial \mathbb{D}_0$ and $\partial \mathbb{D}_a$ (Figure 1). Following Wapenaar et al. (2013), the identity in equation 3 states that when injected as a source field at the top surface $\partial \mathbb{D}_0$, $\mathbf{F}_1^+$ produces a purely-downgoing field that focuses at each point on $\partial \mathbb{D}_a$ at depth.

In the practice of Marchenko redatuming, the only known quantity is $\mathbf{R}$, which is given by the complete reflection response due to all sources and receivers on top of the real medium (e.g., Figure 1a). Both of the $\mathbf{G}^\pm$ responses and focusing functions $\mathbf{F}_1^{+,-}$ are unknown, and the purpose of Marchenko redatuming is to estimate these quantities from the input reflection data $\mathbf{R}$. To accomplish this task, the Marchenko scheme (Broggini et al., 2011; Wapenaar et al., 2013) relies on two other elements in addition to the reflection data: a separation operator Θ and an initial focusing function $\mathbf{F}_{1,0}^+$. The initial $\mathbf{F}_{1,0}^+$ function is such that the desired $\mathbf{F}_1^+ = \mathbf{F}_{1,0}^+ + \mathbf{F}_{1,m}^+$, where $\mathbf{F}_{1,m}^+$ is to be updated by the scheme. Assuming the separation operator satisfies $\Theta \mathbf{G}^- = \mathbf{0}$, $\Theta \mathbf{G}^{+\star} = \mathbf{0}$, $\Theta \mathbf{F}_1^- = \mathbf{F}_1^-$, and $\Theta \mathbf{F}_{1,0}^+ = \mathbf{0}$, then once applied to equations 1 and 2, it yields

$$\mathbf{F}_1^- = \Theta \mathbf{R} \left[\mathbf{F}_{1,0}^+ + \mathbf{F}_{1,m}^+ \right] \,, \tag{4}$$

and

$$\mathbf{F}_{1,m}^+ = \Theta \mathbf{R}^\star\,\mathbf{F}_1^- \,. \tag{5}$$

The system formed by equations 4 and 5 comprises Fredholm integrals of the second kind, which can be solved by means of Neumann series expansions (Kato, 1982). This result yields an iterative solution of the Marchenko system, where K-order solutions to the focusing functions are given by

$$\mathbf{F}_1^{+(K)} = \Omega_K \mathbf{F}_{1,0}^+ \text{ and } \mathbf{F}_1^{-(K)} = \Theta \mathbf{R} \Omega_K \mathbf{F}_{1,0}^+ \,, \tag{6}$$

with the series kernels

$$\Omega_K = \sum_{k=0}^{K} (\Theta \mathbf{R}^\star \Theta \mathbf{R})^k \,. \tag{7}$$

Note that equation 6 shows that the retrieval of $\mathbf{F}_1^+$ is the central step in the iterative Marchenko scheme, since it follows

Inverse transmission in Marchenko redatuming
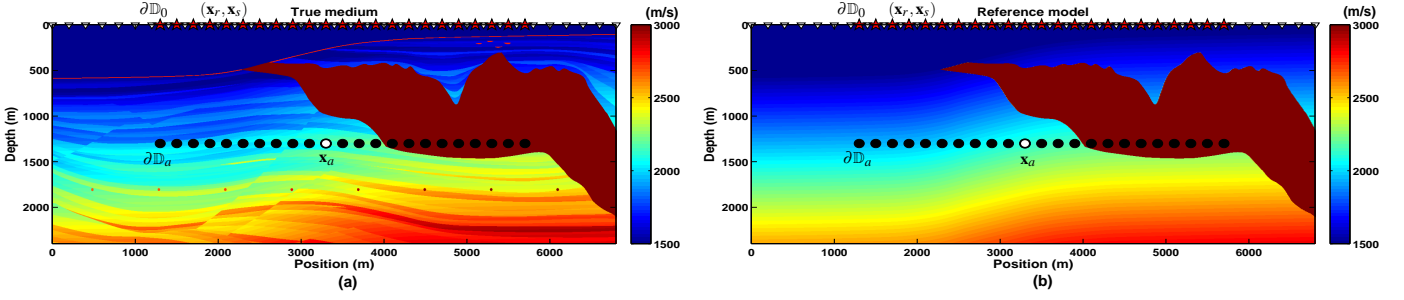
Figure 1: Acquisition geometry and wavespeed models used for Marchenko redatuming. Sources at $\mathbf{x}_s$ and receivers $\mathbf{x}_r$ are placed on the top surface $\partial\mathbb{D}_0$, whereas $\partial\mathbb{D}_a$ represents an arbitrary surface at depth where the redatuming locations $\mathbf{x}_a$ lie. (a) The true model where the reflection data $\mathbf{R}$ are acquired, corresponding also to the desired redatumed fields $\mathbf{p}^{+,-}$. (b) The reference model used to generate the transmission and reflection responses, $\mathbf{T}_{A,0}$ and $\mathbf{R}_{A,0}$, necessary for the Marchenko scheme. Density is constant at 1000 kg/m^3. For $\mathbf{R}$, we model 221 shots, each recorded by 221 receivers. Shot and receiver lines coincide, starting at 1300 m with a 20-m increment. For transmission responses, sources share the same lateral configuration, but are instead placed at a depth of 1300 m.

that $\mathbf{F}_1^{-(K)} = \Theta\mathbf{R}\mathbf{F}_1^{+(K)}$. Finally, the $\mathbf{F}_1^+$ and $\mathbf{F}_1^-$ estimates from equation 6 can be inserted into equations 1 and 2 to yield K-order estimates of the desired redatumed fields $\mathbf{G}^+$ and $\mathbf{G}^-$.

In this paper, we revisit the scheme described by Wapenaar et al. (2014a) by modifying the input $\mathbf{F}_{1,0}^+$ function to accommodate highly complex media. Throughout this paper, our choice for Θ is the same traveltime-based windowing approach used in previous versions of the Marchenko scheme (Broggini et al., 2012; Wapenaar et al., 2013).

Transmission inverses in Marchenko redatuming

In principle, it follows from equation 3 that

$$\mathbf{F}_1^+ = \mathbf{T}_A^{-1} = (\mathbf{T}_A^\dagger\mathbf{T}_A)^{-1}\mathbf{T}_A^\dagger = \mathbf{B}_A^{-1}\mathbf{T}_A^\dagger ; \qquad (8)$$

i.e., $\mathbf{F}_1^+$ is by definition an inverse to the transmission response of the real medium truncated between $\partial\mathbb{D}_0$ and $\partial\mathbb{D}_a$ (Figure 1a). Equation 8 denotes $\mathbf{F}_1^+$ in a least-squares sense, where the adjoint $\mathbf{T}_A^\dagger$ can be thought of as a version of $\mathbf{T}_A^{-1}$ "blurred" by the operator $\mathbf{B}_A = \mathbf{T}_A^\dagger\mathbf{T}_A$. As a result, $\mathbf{B}_A^{-1}$ "deblurs" $\mathbf{T}_A^\dagger$; thus, yielding $\mathbf{F}_1^+$.

Because the retrieval of $\mathbf{F}_1^+$ is a key objective of the Marchenko scheme, the true-medium response $\mathbf{T}_A$ is not available at the outset; instead, one begins with a response $\mathbf{T}_{A,0}$ corresponding to a reference medium. In previous forms of the Marchenko scheme (e.g., Wapenaar et al., 2014a), $\mathbf{T}_{A,0}$ is taken from a smooth velocity model, and $\mathbf{F}_{1,0}^+ = \mathbf{T}_{A,0}^\dagger$ is chosen so that, e.g.,

$$\mathbf{F}_{1,adj}^{+(K)} = \Omega_K\mathbf{T}_{A,0}^\dagger = \Omega_K(\mathbf{B}_{A,0}\mathbf{T}_{A,0}^{-1}) \qquad (9)$$

results from the iterative scheme (equation 6), which is shown to ignore the effect of $\mathbf{B}_{A,0}$ in the theorically desired $\mathbf{F}_{1,0}^+$ (equation 8). Wapenaar et al. (2014a) shows that when the reference medium for $\mathbf{T}_{A,0}$ is smooth, the structure of $\mathbf{B}_{A,0}$ approaches that of an identity matrix, and thus $\mathbf{T}_{A,0}^\dagger \approx \mathbf{T}_{A,0}^{-1}$, apart from scaling factors.

However, to account for scattering effects in highly complex media such as subsalt, we can draw $\mathbf{T}_{A,0}$ from a reference

model such as that in Figure 1b, which contains large contrasts across sharp interfaces. In that case, the structure of $\mathbf{B}_{A,0}$ is more complex, and thus $\mathbf{T}_{A,0}^{-1} \neq \mathbf{T}_{A,0}^\dagger$ making $\mathbf{T}_{A,0}^\dagger$ a less optimum choice for $\mathbf{F}_{1,0}^+$. Here, based on equations 3 and 8, we choose instead $\mathbf{F}_{1,0}^+ = \mathbf{T}_{A,0}^{-1}$, which yields

$$\mathbf{F}_{1,inv}^{+(K)} = \Omega_K(\mathbf{B}_{A,0}^{-1}\mathbf{T}_{A,0}^\dagger) , \qquad (10)$$

with $\mathbf{F}_{1,inv}^{-(K)} = \Theta\mathbf{R}\mathbf{F}_{1,inv}^{+(K)}$ (equation 6). At this point, the estimate of the deblurring operator $\mathbf{B}_{A,0}^{-1}$ becomes the defining factor in differentiating the result in equation 10 from that in equation 9. While it is possible to estimate a direct numerical inverse of $\mathbf{B}_{A,0}$ (e.g., by Tikhonov regularization), here, we choose instead to apply a physical approximation to that inverse because it yields a more numerically stable result. To accomplish that task, we invoke the identity

$$\mathbf{I} = \mathbf{T}_{A,0}^\dagger\mathbf{T}_{A,0} + \mathbf{R}_{A,0}^\dagger\mathbf{R}_{A,0} , \qquad (11)$$

which enforces power conservation between transmission and reflection responses (Wapenaar and Herrmann, 1996; Wapenaar et al., 2004). This identity allows for an N-order estimate of the inverse of $\mathbf{B}_{A,0}$ to be expressed as the series

$$\mathbf{B}_{A,0}^{-1} = \mathbf{I} + \sum_{n=1}^{N}(\mathbf{R}_{A,0}^\dagger\mathbf{R}_{A,0})^n . \qquad (12)$$

When using this result in equation 10, we obtain

$$\mathbf{F}_{1,inv}^{+(K)} = \mathbf{F}_{1,adj}^{+(K)} + \Omega_K(\sum_{n=1}^{N}(\mathbf{R}_{A,0}^\dagger\mathbf{R}_{A,0})^n)\mathbf{T}_{A,0}^\dagger . \qquad (13)$$

This equation shows that our physical estimate of $\mathbf{B}_{A,0}^{-1}$ in equation 12 yields an estimate of $\mathbf{F}_{1,inv}^{+(K)}$ that is the result from previous Marchenko schemes, $\mathbf{F}_{1,adj}^{+(K)}$, superimposed with a correction term containing $(\mathbf{R}_{A,0}^\dagger\mathbf{R}_{A,0})^n$ for $n \geq 1$.

Inverse transmission in Marchenko redatuming

Subsalt example

For our numerical example, we use the Sigsbee models in Figure 1. The reflection response $\mathbf{R}$ is modeled for source (red stars) and receiver (white triangles) locations on top of the model in Figure 1a. The migration velocity model in Figure 1b is used to obtain the reference transmission $\mathbf{T}_{A,0}$, which is generated using only the medium between the levels $\partial\mathbb{D}_0$ and $\partial\mathbb{D}_a$, with sources at depth (circles in Figure 1b) and receivers on the surface in the same configuration as for $\mathbf{R}$ (see Figure 1). From a slightly smoothed version of the model in Figure 1b, we extract the direct-wave traveltimes between points on $\partial\mathbb{D}_a$ and the surface, which are used to create the muting masks that make up the Θ operator (Wapenaar et al., 2014a).

Waveform modeling is performed by staggered-grid, first-order-PDE, acoustic finite differences with a 20-Hz peak-frequency Ricker wavelet as a source pulse. The source pulse is deconvolved from the modelled data to yield $\mathbf{R}$, but kept in $\mathbf{T}_{A,0}$. One essential detail for the purpose of this paper is that all fields in the equations above are *flux-normalized fields* (Wapenaar, 1998), so that one-way reciprocity relations such as, e.g., those denoted by equation 11 indeed hold. As such, the physical fields output by the finite-difference modeling require normalization by local impedance at $\partial\mathbb{D}_0$ for $\mathbf{R}$ and $\mathbf{R}_{A,0}$, and at $\partial\mathbb{D}_a$ for $\mathbf{T}_{A,0}$. This is particularly important at depth, where the datum $\partial\mathbb{D}_a$ lies over large lateral variations in impedance between sediment and salt. In Figure 2, we show the matrices in the power-conservation relation in equation 11 for $\mathbf{T}_{A,0}$ and $\mathbf{R}_{A,0}$ after impedance normalization, from the model and geometry in Figure 1b. Figure 2a shows that $\mathbf{R}_{A,0}^{\dagger}\mathbf{R}_{A,0}$ is slightly more dominated by signals corresponding to the prominent salt reflections on the right-hand side of the model, while $\mathbf{T}_{A,0}^{\dagger}\mathbf{T}_{A,0}$ in Figure 2b is dominated by sources and receivers on the left side of the model where transmitted waves are less obstructed by the salt body. When superposed (Figure 2c), these two matrices approach the identity predicted by theory (equation 11). At the same time, the result in Figure 2c is not a perfect identity matrix due to the finite aperture of source and receiver arrays and the existence of laterally propagating energy (e.g., salt diffractions), which prevent equation 11 from being numerically exact.

The Marchenko-retrieved fields and corresponding initial focusing functions are shown in Figure 3 for a chosen depth location (white circle in Figure 1). The $\mathbf{p}$ notation for the fields in the Figure denotes convolution of the $\mathbf{G}$-fields with the source wavelet. Moreover, the $\mathbf{p}_S$ field in Figure 3a shows the waves in the true medium that cannot be simulated with the reference model in Figure 1b; thus, being the unknown response we wish to retrieve with the Marchenko estimates in Figures 3b and 3c. The Marchenko estimate in Figure 3b uses the initial focusing function in Figure 3d, which is a column of $\mathbf{F}_{1,0}^{+} = \mathbf{B}_{A,0}^{-1}\mathbf{T}_{A,0}^{\dagger}$ with the deblurring operator given by equation 12 with $n = 2$. Figure 3c is the result of the Marchenko scheme with $\mathbf{F}_{1,0}^{+} = \mathbf{T}_{A,0}^{\dagger}$, where the intial focusing function in Figure 3e is simply the time-reversed version of the field modeled between $\mathbf{x}_a$ and the surface using the reference model. When comparing Figures 3b and 3c, we observe that using the initial function in Figure 3d yields an overall better estimate of the field in Figure 3a: not only does the field in Figure 3b provide an improved amplitude update along the first arrivals, it also retrieves several of the salt-related internal multiples, particularly toward the edges of the gather. Albeit better, the estimate in Figure 3b also contains artifacts not present in Figure 3c.

The differences in the Marchenko estimates stem from the differences in the initial focusing functions in Figures 3d and 3e, which, as equations 6 and 13 show, condition the final iterative estimates of $\mathbf{F}_1^{+,-}$ (Figure 4) that are at the core of the redatuming scheme. When comparing the final focusing functions in Figure 4, we see that most of the arrivals retrieved by means $\mathbf{T}_{A,0}^{\dagger}$, are present in $\mathbf{F}_1^{+,-}$ from $\mathbf{T}_{A,0}^{-1}$, albeit with different relative amplitudes. In addition, and more noticeably in Figure 4a, the fields derived with $\mathbf{T}_{A,0}^{-1}$ contain additional arrivals over the entire gather. By inspecting the initial functions in Figures 3d and 3e, we observe that $\mathbf{F}_{1,0}^{+}$ from $\mathbf{T}_{A,0}^{-1}$ contains energy at times past the direct arrival in $\mathbf{T}_{A,0}^{\dagger}$, but is also noticeably different before the direct arrivals as well. The presence of physical energy in $\mathbf{F}_{1,0}^{+}$ before the direct arrivals in Figure 3d violates the condition $\Theta\mathbf{F}_{1,0}^{+} = \mathbf{0}$ (equations 4 and 5) when Θ is the windowing operator described by, e.g., Wapenaar et al. (2014a). The design of an alternative Θ operator to account for the complexity of $\mathbf{F}_{1,0}^{+}$ is the subject of ongoing research.

Conclusions

In this paper, using a compact matrix-based formalism for the Marchenko equations, we review the main elements of the Marchenko iterative scheme while showing that the iterative reconstruction of the downgoing focusing function at depth is the central step of the method. The retrieval of this focusing operator relies on seismic reflection data, together with a data separation filter and an initial/reference focusing function which are in turn drawn from a reference model. Here, we study the role of the initial focusing function, by showing that the initial focusing function chosen in previous Marchenko schemes, while suitable for relatively simple models, has limitations in highly complex models such as subsalt, particularly when the reference model contains large parameter contrasts and sharp interfaces.

To handle more complex subsurface scenarios, we propose the use of alternative initial focusing functions based on the inverse of transmission responses extracted from a reference model (e.g., conventional migration models). We provide a formalism that accounts for such improved focusing functions, and discuss its relationship with previous versions of the Marchenko scheme. In addition, we offer a reflection-based physical approximation to the inverse transmission matrices that yields stable numerical solutions while discussing its implementation details. Using a subsalt numerical example, we demonstrate that the new focusing functions provide improved estimates of subsurface wavefields, with higher first-arrival amplitude fidelity and by successfully retrieving a greater number of internal multiple reflections. Finally, we also point out that this new scheme produces some artifact arrivals, which are could be associated with using the time-domain windowing employed by the original Marchenko approaches.

Inverse transmission in Marchenko redatuming
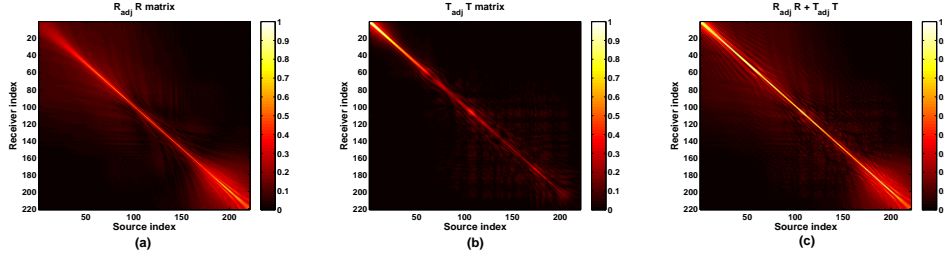
Figure 2: Discrete matrices corresponding to the identity in equation 11 for the reference model in Figure 1b, at a fixed frequency of 20 Hz. (a) The power of $\mathbf{R}_{A,0}^{\dagger}\mathbf{R}_{A,0}$, (b) the power of $\mathbf{T}_{A,0}^{\dagger}\mathbf{T}_{A,0}$ and (c) the superposition of panels (a) and (b). Here, all matrices are normalized by the maximum power of the $\mathbf{T}_{A,0}^{\dagger}\mathbf{T}_{A,0}$ matrix in (b).
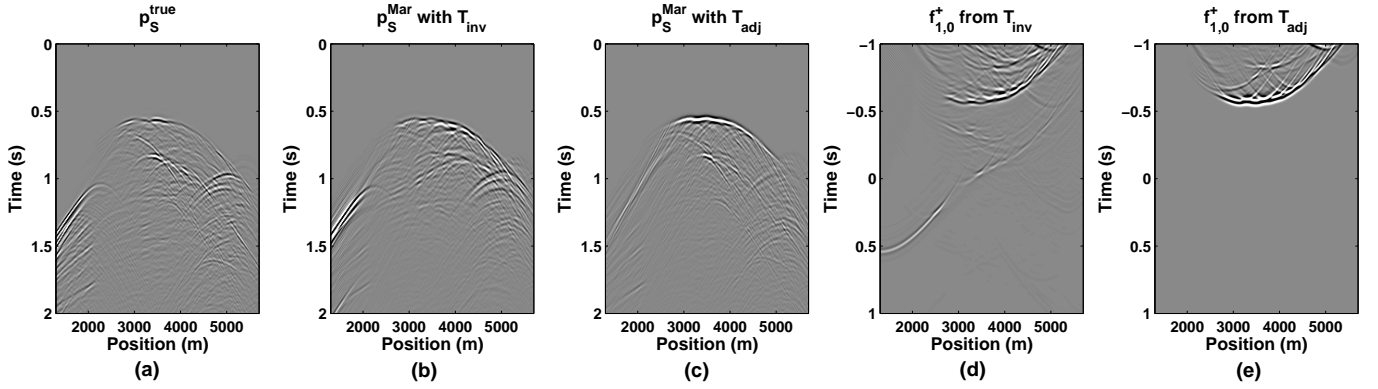
Figure 3: Comparison between true and Marchenko-estimated subsurface fields, along with initial focusing functions. The fields in panels (a) and (b) represent pressure responses for a source at $\mathbf{x}_a$ (white circle in Figure 1) and receivers on the surface. The field $\mathbf{p}_S^{true}$ in (a) is the difference between the full pressure field using the true model in Figure 1a and the reference pressure field using the model in Figure 1b. The responses in (b) and (c) are the result of the superposition of up- and downgoing fields from Marchenko redatuming, i.e., $\mathbf{p}^+ + \mathbf{p}^-$, minus the reference pressure field using the model in Figure 1b. The Marchenko field in (b) results from using an estimate of the inverse transmission operator $\mathbf{T}_{A,0}^{-1}$, while the field in (c) is obtained by the original Marchenko scheme using the adjoint operator $\mathbf{T}_{A,0}^{\dagger}$. The initial focusing functions are illustrated by panels (d) and (e), which represent $\mathbf{F}_{1,0}^+$ between a fixed $\mathbf{x}_a$ (white circle in Figure 1b) and the surface, from $\mathbf{T}_{A,0}^{-1}$ and $\mathbf{T}_{A,0}^{-1}$, respectively.
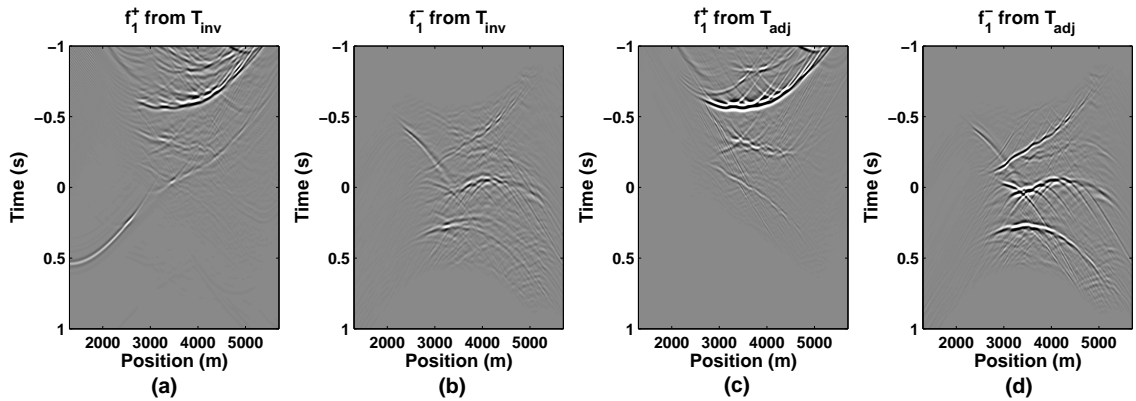
Figure 4: Final focusing functions after four iterations of the Marchenko scheme (equation 6). (a) and (b) show the time-domain version of $\mathbf{F}_1^+$ and $\mathbf{F}_1^-$ for a fixed $\mathbf{x}_a$ (white circle in Figure 1a), that result from using the inverse transmission operator $\mathbf{T}_{A,0}^{-1}$ as the initial focusing function. Analogously, the fields in (c) and (d) result from the adjoint transmission operator $\mathbf{T}_{A,0}^{\dagger}$ as the initial focusing function.